



1 **Multifractal characteristic-based comparison of elements in**
2 **soils within the Daxing and Yicheng areas of Hefei, Anhui**
3 **Province, China**

4 Xiaohui Li^{1,3}, Feng Yuan^{2,1*}, Simon M. Jowitt⁴, Xianglin Li¹, Taofa Zhou^{1,3}, Jie
5 Zhou^{1,3}, Xunyu Hu^{1,3}, Yang Li^{1,3}

6 1. School of Resources and Environmental Engineering, Hefei University of
7 Technology, Hefei 230009, China

8 2. Xinjiang Research Centre for Mineral Resources, Xinjiang Institute of Ecology and
9 Geography, Chinese Academy of Sciences, Urumqi, Xinjiang 830011, China

10 3. Ore Deposit and Exploration Centre, Hefei University of Technology, Hefei
11 230009, China

12 4. School of Earth, Atmosphere and Environment, Monash University, Wellington
13 Road, Clayton, VIC 3800, Australia

14 *Corresponding author: Email: yf_hfut@163.com, Tel: +8605512901648

15 **Abstract**

16 Industrial and agricultural activities can generate heavy metal pollution that can
17 have a number of negative environmental and health impacts. This means that
18 identifying areas with heavy metal pollution and the sources of these pollutants,
19 especially in urban or developed areas with multiple possible sources of pollution, is
20 an important first step in mitigating the effects of these contaminating but necessary
21 economic activities. Here, we present the results of a heavy metal (Cu, Pb, Zn, Cd, As
22 and Hg) soil geochemical survey and outline a new multifractal characteristic-based
23 comparison method that allows deeper interrogation of soil geochemistry in urban or
24 developed areas. This survey focuses on Hefei, the provincial capital of Anhui
25 Province, China, an area that contains a number of individual towns within a large



26 municipal area. This study focuses on the towns of Daxing and Yicheng both of which
27 are incorporated within Hefei and are economically focused on industry and
28 agriculture, respectively. Here, we use a multifractal spectral technique to identify
29 differences in the geochemistry of soils within the Daxing and Yicheng areas. The
30 height difference between the two ends of the multifractal spectrum of the
31 geochemical data ($\Delta f(a)$) for soils in the Daxing area decreases as follows:
32 Pb>As>Cd>Cu>Zn>Hg, whereas $\Delta f(a)$ values of the geochemical data for soils in the
33 Yicheng town areas decreases as follows: Hg>Zn>As>Cd>Pb>Cu. These differences
34 indicate that the soils in these areas have differing multifractal geochemical
35 characteristics, suggesting that the differing economic activities in these areas
36 generate distinctly different heavy metal pollutant loads (e.g. Hg dominated
37 agricultural pollution vs. Pb dominated industrial pollution). In addition, all of the
38 elements barring Hg have larger $\Delta f(a)$ values in the Daxing area compared to the
39 Yicheng area. These larger ranges indicate that the higher concentrations of heavy
40 metals present in soils within the Daxing area (compared to the Yicheng area) are
41 more likely to be related to industrial activities than agriculture. The industrial Daxing
42 area contains significant Pb and As soil contamination, whereas Hg is the main heavy
43 metal present in soils within the Yicheng area, indicating that differing clean-up
44 procedures and approaches to remediating these polluted areas are needed, rather than
45 a single approach to heavy metal pollution. The research presented here also
46 highlights that the soils in these areas (and the source of these pollutants) need to be
47 remedied in order to avoid further health and environmental impacts.

48 **Keywords:** soil geochemistry; multifractal modelling, heavy metal pollution, Hefei.

49

50 1. Introduction

51 Multifractal based analytical techniques have recently been used in a number of
52 differing fields, including geophysics (Schertzer et al., 2011), medicine (Jennane et al.,
53 2001), computer science (Wendt et al., 2009), geology (Deng et al., 2011; Zuo et al.,
54 2012; Cheng, 1995; Yuan et al., 2012), environmental science (Lima et al., 2003;



55 Albanese et al., 2007; Guillén et al., 2011; Salvadori et al., 1997), and ecology
56 (Scheuring and Riedi, 1994; Pascual et al., 1995) among others. The advantages of
57 these multifractal techniques include the fact that these approaches can identify
58 non-linear characteristics, yielding new information that can be used to understand the
59 controls on the distribution of key elements within the objects or data being studied
60 (Gonçalves, 2000; Zuo et al., 2012). Multifractal techniques can also be used to
61 analyze soil characteristics, including the identification of porous structures and the
62 spatial variability in the characteristics of soils (Dathe et al., 2006; Caniego et al.,
63 2005). These techniques can also enable the characterization of complex
64 phenomena in the spatial distribution of elements within soils, improving our
65 knowledge of the controls on the geochemistry of soils and the regolith (Gonçalves,
66 2000). This means that these approaches can not only be used in mineral exploration
67 (Yuan et al., 2012; Yuan et al., 2015; Zuo, 2014; Nazarpour et al., 2014) but can also
68 be used in the analysis of pollutants such as heavy metals within soils (Guillén et al.,
69 2011; Salvadori et al., 1997). Heavy metal pollution poses a serious risk for human
70 health and the environment, meaning that soil pollution caused by anthropogenic
71 activities (including industry and agriculture) has been the focus of a significant
72 amount of research in recent years (McGrath et al., 2004; Wang et al., 2007; Leyval et
73 al., 1997; Thomas and Stefan, 2002; Chunling et al., 2011). This in turn indicates that
74 multifractal techniques enable the more precise identification of areas of
75 contamination and the degree of contamination in polluted areas. Multifractal
76 techniques, such as singularity mapping and multifractal interpolation, also enable
77 more detailed analysis of the spatial distribution of heavy metals by the use of C–A
78 models to define threshold values between background (i.e. geological) and
79 anthropogenic anomalies, S–A modeling that uses these thresholds to spatially
80 separate anomalies (i.e., anthropogenically derived heavy metal concentrations in this
81 case) from background concentrations (i.e., geologically derived heavy metal
82 concentrations), and using multifractal spectra to highlight non-linear characteristics
83 and identify anomalous behavior that reflects the characteristics of some multifractal



84 sets (Gonçalves, 2000; Albanese et al., 2007; Guillén et al., 2011; Lima et al., 2003;
85 Cheng, 2001).

86 Hefei is the provincial capital of Anhui Province, China, and has an urban area
87 that includes the towns of Daxing and Yicheng, areas that focus on industrial and
88 agricultural activity, respectively. These towns provide an ideal location to compare
89 and contrast the degree and characteristics of any heavy metal contamination of soils
90 associated with these anthropogenic activities. This study focuses on these areas, and
91 the results presented here further our understanding of any heavy metal pollution that
92 is likely associated with these differing activities, both enabling and informing future
93 planning for any necessary remediation of these soils. Our study uses multifractal
94 techniques to determine the multifractal characteristics of the distribution of heavy
95 metals in soils in these areas, enabling the characterization and contrasting of the
96 heavy metal pollution of soils in these two towns.

97 **2. Study area and geochemical data**

98 **2.1 Study area**

99 The city of Hefei is situated in central–eastern China (Fig. 1(a)), has
100 approximately 7.7 million inhabitants and covers an area of around 11,408 km². This
101 paper focuses on the towns of Daxing and Yicheng (Fig. 1(b)), with the former
102 representing one of the traditional industrial bases of the Hefei area and containing
103 numerous industrial factories that are involved in the steel industry, chemical industry,
104 paper making, and the production of furniture and construction materials, amongst
105 others. In contrast, the town of Yicheng is agricultural, with the economy of the town
106 focused on agricultural production, byproduct processing, livestock and poultry
107 breeding, flower planting, and other enterprises related to agricultural activity.

108 **2.2 Sampling and analysis**

109 The study areas are covered by Quaternary sedimentary soils and are free of both
110 natural mineralization and mining activities. A total of 169 surface (<20 cm below
111 surface) soil samples were taken from the towns of Daxing and Yicheng on 1 × 1 km
112 grids, yielding 78 samples from Daxing and 91 samples from Yicheng (Fig. 1(c–d)).



113 Sampling errors were minimized by splitting each sample into 3–5 sub-samples, each
114 of which weighed more than 500 g. Each of these sub-samples was dried in air before
115 being broken up using a wooden roller and then sieved to pass through a 0.85 mm
116 mesh. The concentrations of 6 heavy metal elements (Cu, Pb, Zn, Cd, As and Hg) in
117 the soil samples described above were determined during this study. Cd, Cu, Pb and
118 Zn concentrations were determined by inductively coupled plasma–mass spectrometry
119 (ICP–MS), with Hg and As concentrations determined by hydride generation–atomic
120 fluorescence spectrometry (AFS). These techniques have detection limits of 1 ppm for
121 Cu, 2 ppm for Pb and Zn, 30 ppb for Cd, 0.5 ppm for As and 5 ppb for Hg. The
122 accuracy of these analyses was monitored by repeat analysis of standards and
123 replicate analyses of sub-sets of samples using instrumental neutron activation
124 analysis (INAA). Analytical precision was monitored using analysis of variance of the
125 results obtained from duplicate analyses.

126 **2.3 Results**

127 The results of a statistical analysis of the resulting soil geochemical data are
128 given in Table 1. Samples from Daxing have higher Cu, Pb, Zn, Cd and As maximum,
129 standard deviation, skewness, and kurtosis values than soil samples from the Yicheng
130 area. In addition, the soil samples from Daxing have much higher coefficient of
131 variation (CV) values for Cu, Pb, Zn, Cd and As than the samples from the Yicheng
132 area, indicating that soils in the Daxing area contain much higher and more variable
133 concentrations of these elements. This suggests that samples from the Daxing area
134 with elevated concentrations of heavy metals beyond the natural background
135 variations in these areas were probably contaminated by anthropogenic activity.

136 All of the elements (barring Cu in the Yicheng area) in both the Yicheng and
137 Daxing areas yield histograms that are positively skewed and contain some outliers,
138 indicating that these data have non-normal, fractal-, or multifractal-type distributions.
139 This means that multifractal techniques may be more suitable for the characterization
140 of the geochemistry of the contaminated soils in these areas (Fig. 2).

141



142 3. Multifractal spectrum analysis

143 Multifractal formalisms can decompose self-similar measures into intertwined
144 fractal sets that are characterized by singularity strength and fractal dimensions
145 (Cheng, 1999). Using multifractal techniques allows non-linear characteristics within
146 datasets to be identified, enabling the extraction of information that can be used to
147 understand the controls on the distribution of key elements within data. Fractal spectra
148 ($f(a)$) are multifractal formalisms that can be used to describe the multifractal
149 characteristics of a dataset and can be estimated using box-counting based moment,
150 gliding box, histogram and wavelet methods, among others (Cheng, 1999; Lopes and
151 Betrouni, 2009). The most widely used of these methods of estimating $f(a)$ values are
152 the box-counting and gliding box methods, both of which are based on the moment
153 method.

154 The initial step of the box-counting method estimates mass exponent function $\tau(q)$
155 values using a partition function as follows (Halsey et al., 1986):

$$156 \quad \tau(q) = \lim_{\varepsilon \rightarrow 0} \left(\frac{\log(\chi^q(\varepsilon))}{\log(\varepsilon)} \right) = \lim_{\varepsilon \rightarrow 0} \left(\frac{\log \sum_{i=1}^{N(\varepsilon)} \mu_i^q(\varepsilon)}{\log(\varepsilon)} \right)$$

157 where $\mu_i(\varepsilon)$ denotes a measure with the i_{th} box of size ε and $N(\varepsilon)$ indicates the total
158 number of boxes of size ε with $\mu_i(\varepsilon)$ values that $\neq 0$.

159 The calculation of the mass exponent function $\tau(q)$ for the gliding box method is
160 different from the box-counting method, with the gliding box method providing a
161 useful approach that can increase the number of samples within a dataset that are
162 available for statistical estimation (Tarquis et al., 2006; Xie et al., 2010; Buczkowski
163 et al., 1998). This means that the gliding box approach often provides better results
164 with lower uncertainties than the box-counting method (Cheng, 1999). As such, we
165 have used the gliding box approach during this study.

166 The calculation of the mass exponent function $\tau(q)$ for the gliding box method
167 uses a partition function as follows (Cheng, 1999):



$$\langle \tau(q) \rangle + D = \lim_{\varepsilon \rightarrow 0} \left(\frac{\log(\mu^q(\varepsilon))}{\log(\varepsilon)} \right) = \lim_{\varepsilon \rightarrow 0} \left(\frac{\log(1/N^*(\varepsilon)) \sum_{i=1}^{N^*(\varepsilon)} \mu_i^q(\varepsilon)}{\log(\varepsilon)} \right)$$

where $\mu_i(\varepsilon)$ denotes a measure with the i_{th} cell of a gliding box of size ε , $\langle \rangle$ indicates the statistical moment, and $N^*(\varepsilon)$ indicates the total number of gliding boxes of size ε with $\mu_i(\varepsilon)$ values that $\neq 0$.

The values of $\tau(q)$ derived using this equation can be then used to determine α and $f(a)$ values using a Legendre transformation, as expressed below:

$$\alpha(q) = \frac{d\tau(q)}{dq}$$

$$f(q) = q\alpha(q) - \tau(q) = q \frac{d\tau(q)}{dq} - \tau(q)$$

where $\Delta\alpha$ and Δf are essential parameters required to analyze the multifractal characteristics of the dataset in question. The widths of the left and right branches within the multifractal spectra are then defined using the following equations:

$$\Delta\alpha_L = \alpha_0 - \alpha_{\min}$$

$$\Delta\alpha_R = \alpha_{\max} - \alpha_0$$

$$\Delta\alpha = \alpha_{\max} - \alpha_{\min}$$

and the height difference $\Delta f(a)$ between the two ends of the multifractal spectrum are then extracted using:

$$\Delta f(\alpha) = f(\alpha_{\max}) - f(\alpha_{\min})$$

Higher Δa and $\Delta f(a)$ values are generally indicative of datasets with heterogeneous distribution patterns and higher levels of multifractality (Cheng, 1999; Kravchenko et al., 1999). In addition, multifractality associated with ordinary spatial analysis parameters, as represented by the $\tau''(1)$ parameter, can also be used to quantitatively characterize the multifractality of a dataset (Cheng, 2006) using the following equation:

$$\tau''(1) = \tau(2) - 2\tau(1) + \tau(0)$$



192 4. Calculation processes and discussion

193 The gliding box method used during this study can increase the number of
194 samples that can be used in statistical estimations and provides results with lower
195 uncertainties than the box-counting method. This, combined with the relatively sparse
196 sample locations used in this study, means that we used the gliding box method to
197 calculate multifractal spectra values for the geochemical data from the study area.
198 This calculation used a range of q values from -10 to 10 with an interval of 1 ,
199 yielding the multifractal analytical results given in Table 2 and the multifractal spectra
200 (in the form of an α - $f(\alpha)$ diagram) shown in Fig. 3.

201 The multifractal data shown in Table 2 indicate that all of the elements barring Cu
202 and Pb in the Yicheng area are characterized by a wide range of α values (i.e. have
203 high $\Delta\alpha$ values) and have $\tau''(1)$ values less than -0.01 . In addition, these data have a
204 wider range of $\Delta f(\alpha)$ values compared to the $\Delta\alpha$ and $\tau''(1)$ values shown in Table 2.
205 This means that the $\Delta f(\alpha)$ values obtained from these data may be the best measure to
206 determine the multifractal characteristics of the distribution of these elements in soils
207 within the study area.

208 The range of $f(\alpha)$ values for the geochemical data for soils within the Daxing area
209 decreases in the order: Pb>As>Cd>Cu>Zn>Hg, whereas the values for these elements
210 in soils within the Yicheng area decreases in the order: Hg>Zn>As>Cd>Pb>Cu,
211 indicating a significant difference in the geochemical characteristics (and heavy metal
212 pollution) in the soils within these two areas. These variations are linked to
213 multifractal spectra (shown as an α - $f(\alpha)$ plot in Fig. 3), where combining the
214 singularity exponent α and the corresponding fractal dimension $f(\alpha)$ generates a
215 multifractal spectrum with an inverse bell shape. All of these spectra (barring the data
216 for Cu in soils from the Yicheng area) show a steep increase (i.e. have a good positive
217 correlation between the values) followed by a shorter section of the curve where these
218 values negatively correlate (Fig. 3). All of these data are also asymmetric with respect
219 to α for all elements, indicating that soils containing low and high concentrations of
220 these elements are not evenly distributed within the study area (as is expected for



221 areas containing point source pollutants like factories or individual farms).

222 All of the heavy metals analyzed during this study barring Hg have higher $\Delta f(\alpha)$
223 values in soils from the Daxing area, with Hg having higher values in soils from the
224 Yicheng area (Table 2). This suggests that the industrial activities in the Daxing area
225 generate multi-element heavy metal contamination soil contamination, whereas the
226 only significant heavy metal pollution associated with the agricultural activity in the
227 Yicheng area is Hg contamination. However, the Hg $\Delta f(\alpha)$ values in Yicheng area are
228 larger than all of the other elements in this area as well as some of the elements in the
229 Daxing area, indicating both the prevalence and significant degree of agricultural Hg
230 contamination in the Yicheng area. This is important, primarily as Hg pollution
231 can seriously impact human health as this element is concentrated upward in the food
232 chain (e.g. (Jiang et al., 2006)), meaning that this contamination needs to be evaluated
233 further and remediated to avoid any deleterious effects.

234 We further analyzed the spatial distribution of contamination within soils
235 from the Daxing and Yicheng areas by examining the elements with the highest $\Delta f(\alpha)$
236 values, namely Pb and Hg, respectively. We used an approach focused on filled
237 contour maps showing the distribution of Pb in the Daxing area and Hg in the Yicheng
238 area using inverse distance weighted interpolation (Fig. 4–5). These maps indicate
239 that areas with elevated levels of Pb contamination within the Daxing area are directly
240 correlated to the location of industrial factories, whereas the Hg contamination in the
241 Yicheng area is spatially correlated with the location of agricultural breeding facilities.
242 This strongly suggests that the larger $\Delta f(\alpha)$ values for these elements within the
243 geochemical data are related to the industrial and agricultural activities in the Daxing
244 and Yicheng areas, respectively. The Hg contamination in the Yicheng area is of
245 significance, especially as this form of contamination can cause serious health issues
246 (e.g. Minamata disease). As such, the soils in this area may well require remediation,
247 especially as Hg can be concentrated up the food chain and the Yicheng area is
248 heavily agricultural, indicating that this activity may both be concentrating Hg as well
249 as contaminating soils in this area. This distribution of soils with elevated
250 concentrations of Hg also contrasts with the symmetrical distribution and relatively



251 low $\Delta f(\alpha)$ values for Cu within the Yicheng area (Fig. 3). Comparing the distribution
252 of Cu and Hg in the filled contours maps for the Yicheng area (Fig. 5–6) indicates an
253 anti-correlation in terms of the spatial location of anomalously high concentrations of
254 Cu and breeding facilities. This indicates that little Cu has been anthropogenically
255 added (or removed) from the soils in the Yicheng area, suggesting that these soils
256 maybe contain only natural background concentrations of Cu and that the agricultural
257 activity in this area does not produce any significant Cu contamination. These data
258 indicate that differing clean-up procedures and approaches to remediating these
259 polluted areas are needed, rather than a single approach to heavy metal pollution. The
260 results also indicate that multifractal modeling and the associated generation of
261 multifractal parameters, such as $\Delta f(\alpha)$ values, are a useful approach in the evaluation
262 of heavy metal pollution in soils and the identification of major element of heavy
263 metal contamination.

264 5. Conclusions

265 Our data indicate that the soils from the Daxing area have a larger range of $f(\alpha)$
266 values for Cu, Pb, Zn, Cd and As than soils from the Yicheng area, although have a
267 larger range in $f(\alpha)$ values for Hg. The range of $f(\alpha)$ values for the soil geochemical
268 data in the Daxing area decreases in the order Pb>As>Cd>Cu>Zn>Hg, whereas soils
269 in the Yicheng area have $f(\alpha)$ value ranges that decrease in the order
270 Hg>Zn>As>Cd>Pb>Cu. In addition, Cu concentrations in soils in the Yicheng area
271 may still have their original (i.e. natural) distribution and may not have been
272 influenced by human activities. These data indicate that the industrial activity
273 concentrated in the Daxing area generates multi-element heavy metal soil
274 contamination whereas the agricultural activity concentrated in the Yicheng area
275 generates Hg dominated heavy metal soil contamination. The latter is important, as
276 Hg contamination can cause serious health issues (e.g. Minamata disease) and the
277 soils in this area may well require remediation, especially as Hg can be concentrated
278 up the food chain and the Yicheng area is heavily agricultural, indicating that this
279 activity may both be concentrating Hg as well as contaminating soils in this area.



280 The initial results presented here indicate that multifractal modeling and the
281 associated generation of multifractal parameters may be a useful approach in the
282 evaluation of heavy metal pollution in soils and the identification of major sources of
283 of heavy metal contamination. Finally, the fact that $\Delta f(\alpha)$ yield larger differences than
284 compared with the Δa and $\tau''(1)$ value means that $f(\alpha)$ values may be more useful than
285 Δa and $\tau''(1)$ values during the determination of the multifractal characteristics of
286 datasets analyzed using this method.

287

288 **Acknowledgements**

289 This research was financially supported by funds from the Programme for New
290 Century Excellent Talents in University (Grant No. NCET-10-0324), and the China
291 Academy of Science "Light of West China" Program.

292 **References**

- 293 Albanese, S., De Vivo, B., Lima, A., and Cicchella, D.: Geochemical background and
294 baseline values of toxic elements in stream sediments of Campania region (Italy),
295 Journal of Geochemical Exploration, 93, 21-34, 2007.
- 296 Buczkowski, S., Hildgen, P., and Cartilier, L.: Measurements of fractal dimension by
297 box-counting: a critical analysis of data scatter, Physica A Statistical Mechanics &
298 Its Applications, 252, 23–34, 1998.
- 299 Caniego, F. J., Espejo, R., Martín, M. A., and José, F. S.: Multifractal scaling of soil
300 spatial variability, Ecological Modelling, 182, 291-303, 2005.
- 301 Cheng, Q.: The perimeter-area fractal model and its application to geology,
302 Mathematical Geology, 27, 69-82, 1995.
- 303 Cheng, Q.: The gliding box method for multifractal modeling, Comput. Geosci., 25,
304 1073-1079, 1999.
- 305 Cheng, Q. M.: Selection of Multifractal Scaling Breaks and Separation of
306 Geochemical and Geophysical Anomaly, Journal of China university of
307 geosciences, 1, 54-59, 2001.
- 308 Cheng, Q. M.: Multifractal modelling and spectrum analysis: Methods and



- 309 applications to gamma ray spectrometer data from southwestern Nova Scotia,
310 Canada, *Science in China Series D: Earth Sciences*, 49, 283-294, 2006.
- 311 Chunling, L., Chuanping, L., Yan, W., Xiang, L., Fangbai, L., Gan, Z., and Xiangdong,
312 L.: Heavy metal contamination in soils and vegetables near an e-waste processing
313 site, South China, *Journal of hazardous materials*, 186, 481-490, 2011.
- 314 Dathe, A., Tarquis, A. M., and Perrier, E.: Multifractal analysis of the pore- and
315 solid-phases in binary two-dimensional images of natural porous structures,
316 *Geoderma*, 134, 318–326, 2006.
- 317 Deng, J., Wang, Q., Wan, L., Liu, H., Yang, L., and Zhang, J.: A multifractal analysis
318 of mineralization characteristics of the Dayingezhuang disseminated-veinlet gold
319 deposit in the Jiaodong gold province of China, *Ore Geology Reviews*, 40, 54–64,
320 2011.
- 321 Gonçalves, M. A.: Characterization of Geochemical Distributions Using Multifractal
322 Models, *Mathematical Geology*, 33, 41-61, 2000.
- 323 Guillén, M. T., Delgado, J., Albanese, S., Nieto, J. M., Lima, A., and De Vivo, B.:
324 Environmental geochemical mapping of Huelva municipality soils (SW Spain) as
325 a tool to determine background and baseline values, *Journal of Geochemical
326 Exploration*, 109, 59-69, 2011.
- 327 Halsey, T.C., Jensen, M.H., Kadano, L.P., Procaccia, I., and Shraiman, B.I.: Fractal
328 measures and their singularities: the characterization of strange sets. *Physical
329 Review*, A, 33 (2), 1141-1151, 1986.
- 330 Jennane, R., Ohley, W. J., Majumdar, S., and Lemineur, G.: Fractal analysis of bone
331 X-ray tomographic microscopy projections, *IEEE Transactions on Medical
332 Imaging*, 20, 443-449, 2001.
- 333 Jiang, G. B., Shi, J. B., and Feng, X. B.: Mercury Pollution in China, *Environmental
334 Science & Technology*, 40, 3672-3678, 2006.
- 335 Kravchenko, A., Boast, C., and Bullock, D.: Multifractal analysis of soil spatial
336 variability, *Agronomy Journal*, 91, 1033-1041, 1999.
- 337 Leyval, C., Turnau, K., and Haselwandter, K.: Effect of heavy metal pollution on
338 mycorrhizal colonization and function: physiological, ecological and applied



- 339 aspects, *Mycorrhiza*, 7, 139-153, 1997.
- 340 Lima, A., De Vivo, B., Cicchella, D., Cortini, M., and Albanese, S.: Multifractal IDW
341 interpolation and fractal filtering method in environmental studies: an application
342 on regional stream sediments of (Italy), Campania region, *Applied Geochemistry*,
343 18, 1853-1865, 2003.
- 344 Lopes, R., and Betrouni, N.: Fractal and multifractal analysis: A review, *Medical*
345 *Image Analysis*, 13, 634-649, 2009.
- 346 McGrath, D., Zhang, C., and Carton, O. T.: Geostatistical analyses and hazard
347 assessment on soil lead in Silvermines area, Ireland, *Environmental Pollution*,
348 127, 239-248, 2004.
- 349 Nazarpour, A., Omran, N. R., Paydar, G. R., Sadeghi, B., Matroud, F., and Nejad, A.
350 M.: Application of classical statistics, logratio transformation and multifractal
351 approaches to delineate geochemical anomalies in the Zarshuran gold district,
352 NW Iran, *Chemie der Erde - Geochemistry*, 75, 117-132, 2014.
- 353 Pascual, M., Ascioti, F., and Caswell, H.: Intermittency in the plankton: a multifractal
354 analysis of zooplankton biomass variability, *Journal of Plankton Research*, 17,
355 167-168, 1995.
- 356 Salvadori, G., Ratti, S. P., and Belli, G.: Fractal and multifractal approach to
357 environmental pollution, *Environmental Science & Pollution Research*, 4, 91-98,
358 1997.
- 359 Schertzer, D., Lovejoy, S., Schmitt, F., Chigirinskaya, Y., and Marsan, D.: Multifractal
360 Cascade Dynamics and Turbulent Intermittency, *Fractals-complex Geometry*
361 *Patterns & Scaling in Nature & Society*, 5, 427-471, 2011.
- 362 Scheuring, I., and Riedi, R.: Application of multifractals to the analysis of vegetation
363 pattern, *Journal of Vegetation Science*, 5, 489-489, 1994.
- 364 Tarquis, A. M., Mcinnes, K. J., Key, J. R., Saa, A., Garc á, M. R., and D áz, M. C.:
365 Multiscaling analysis in a structured clay soil using 2D images, *Journal of*
366 *Hydrology*, 322, 236-246, 2006.
- 367 Thomas, K., and Stefan, S.: Estimate of heavy metal contamination in soils after a
368 mining accident using reflectance spectroscopy, *Environmental Science &*



- 369 Technology, 36, 2742-2747, 2002.
- 370 Wang, Y. P., Shi, J. Y., Wang, H., Lin, Q., Chen, X. C., and Chen, Y. X.: The influence
371 of soil heavy metals pollution on soil microbial biomass, enzyme activity, and
372 community composition near a copper smelter. *Ecotox Environ Safe*,
373 *Ecotoxicology & Environmental Safety*, 67, 75-81, 2007.
- 374 Wendt, H., Roux, S. G., Jaffard, S., and Abry, P.: Wavelet leaders and bootstrap for
375 multifractal analysis of images, *Signal Processing*, 89, 1100–1114, 2009.
- 376 Xie, S., Cheng, Q., Xing, X., Bao, Z., and Chen, Z.: Geochemical multifractal
377 distribution patterns in sediments from ordered streams, *Geoderma*, 160, 36-46,
378 2010.
- 379 Yuan, F., Li, X., Jowitt, S. M., Zhang, M., Jia, C., Bai, X., and Zhou, T.: Anomaly
380 identification in soil geochemistry using multifractal interpolation: A case study
381 using the distribution of Cu and Au in soils from the Tongling mining district,
382 Yangtze metallogenic belt, Anhui province, China, *Journal of Geochemical*
383 *Exploration*, 116-117, 28-39, 2012.
- 384 Yuan, F., Li, X., Zhou, T., Deng, Y., Zhang, D., Xu, C., Zhang, R., Jia, C., and Jowitt,
385 S. M.: Multifractal modelling-based mapping and identification of geochemical
386 anomalies associated with Cu and Au mineralisation in the NW Junggar area of
387 northern Xinjiang Province, China, *Journal of Geochemical Exploration*, 154,
388 252-264, 2015.
- 389 Zuo, R., Carranza, E. J. M., and Cheng, Q.: Fractal/multifractal modelling of
390 geochemical exploration data, *Journal of Geochemical Exploration*, 122, 1-3,
391 2012.
- 392 Zuo, R.: Identification of geochemical anomalies associated with mineralization in the
393 Fanshan district, Fujian, China, *Journal of Geochemical Exploration*, 139,
394 170–176, 2014.
- 395
- 396



397 **Table 1.** Statistical analysis of soil geochemical data from the towns of Daxing and Yicheng.

Town	Element	Concentrations						CV* (%)
		Min	Max	Mean	Standard deviation	Skewness	Kurtosis	
Daxing	Cu (mg/kg)	19.00	111.50	33.87	13.26	3.20	14.93	39.16
	Pb (mg/kg)	18.90	291.30	39.57	35.03	5.37	35.41	88.51
	Zn (mg/kg)	40.90	526.10	105.8	94.40	2.91	8.59	89.19
	Cd (mg/kg)	0.045	1.48	0.23	0.24	3.45	13.81	108.23
	As (mg/kg)	4.93	308.20	13.97	33.89	8.72	76.64	242.56
	Hg (mg/kg)	0.03	0.60	0.11	0.11	2.68	7.78	107.29
Yicheng	Cu (mg/kg)	9.60	37.80	24.34	5.77	-0.38	0.41	23.71
	Pb (mg/kg)	10.40	46.30	22.77	4.91	0.87	5.51	21.56
	Zn (mg/kg)	20.80	194.80	54.70	21.43	3.45	20.27	39.17
	Cd (mg/kg)	0.054	0.43	0.15	0.08	1.84	3.49	51.85
	As (mg/kg)	2.30	44.20	7.29	4.39	6.68	56.55	60.24
	Hg (mg/kg)	0.02	0.62	0.06	0.07	5.75	41.26	113.09

398 *CV: coefficient of variation.

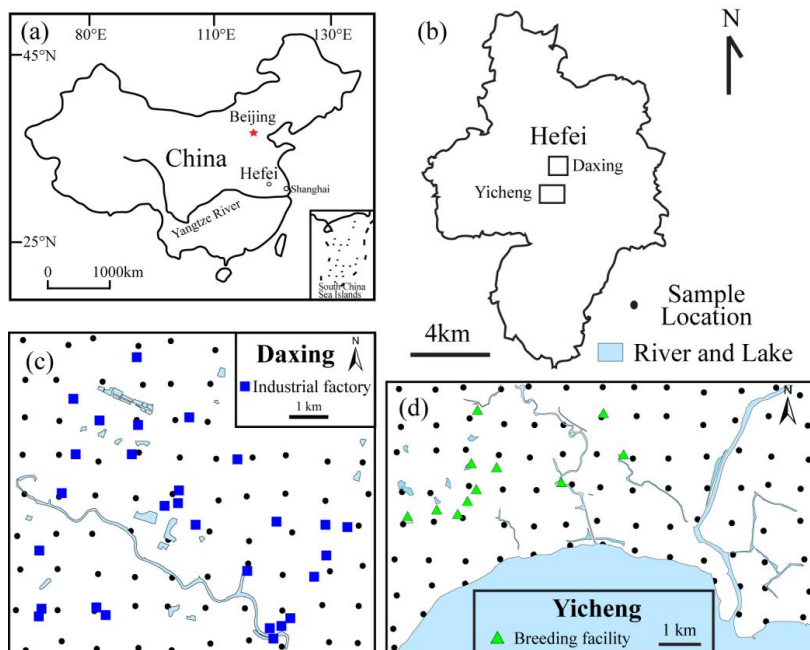
399



400 **Table 2.** Multifractal parameters that describing the multifractality of all of the elements within
 401 the soil samples analyzed during this study.

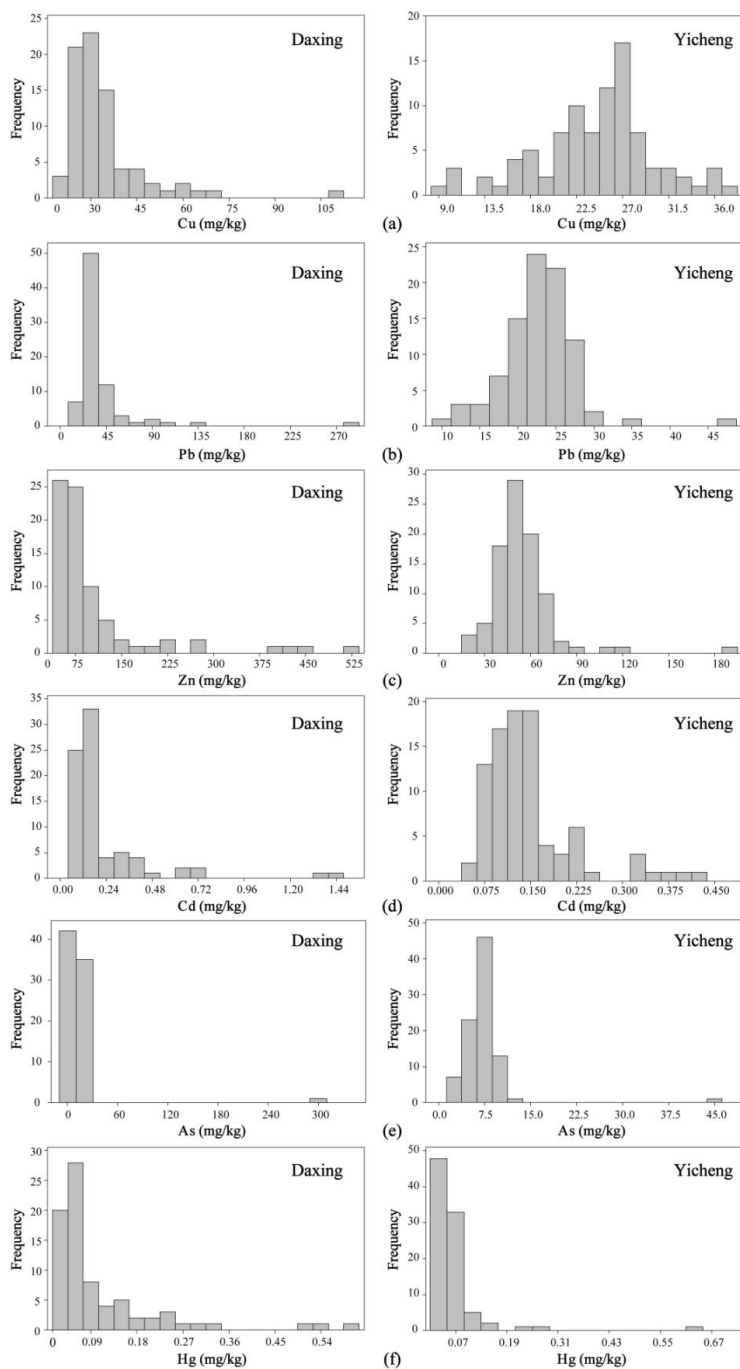
Town	Element	a_{\min}	a_{\max}	Δa_L	Δa_R	Δa	$\Delta f(a)$	$\tau''(\mathbf{1})$
Daxing	Cu	1.733	2.057	0.280	0.044	0.324	1.270	-0.015
	Pb	1.439	2.050	0.567	0.044	0.611	1.659	-0.068
	Zn	1.733	2.109	0.288	0.088	0.376	0.841	-0.066
	Cd	1.482	2.285	0.499	0.304	0.803	1.358	-0.066
	As	1.285	2.094	0.739	0.070	0.809	1.490	-0.243
	Hg	1.780	2.191	0.248	0.163	0.411	0.656	-0.079
Yicheng	Cu	1.971	2.067	0.036	0.060	0.096	0.168	-0.007
	Pb	1.900	2.062	0.104	0.058	0.162	0.646	-0.005
	Zn	1.729	2.112	0.275	0.108	0.383	1.275	-0.016
	Cd	1.800	2.103	0.201	0.102	0.303	0.829	-0.023
	As	1.659	2.076	0.343	0.075	0.418	1.224	-0.036
	Hg	1.507	2.084	0.497	0.080	0.577	1.243	-0.096

402

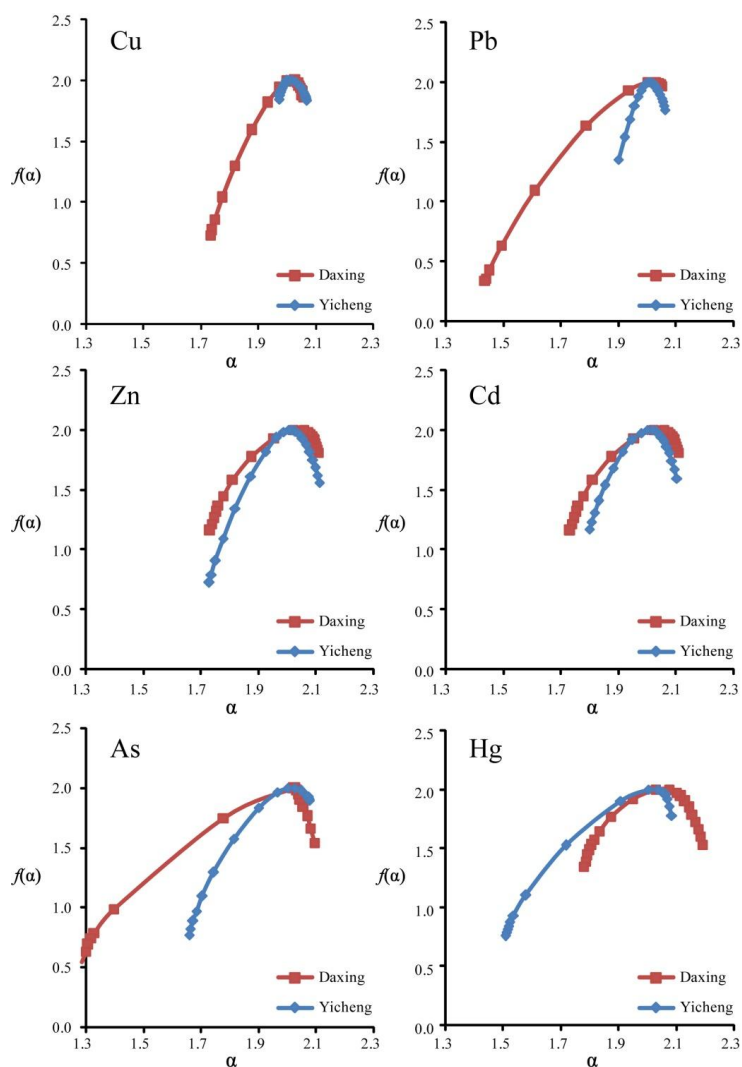


403

404 **Fig.1.** (a) Map showing the location of Hefei in central-eastern China; (b) Map showing the
405 location of the study areas within Hefei; (c) Map showing the location of soil samples taken in a 1
406 x 1 km grid in the town of Daxing; (d) Map showing the location of soil samples taken in a 1 x 1
407 km grid in the town of Yicheng.



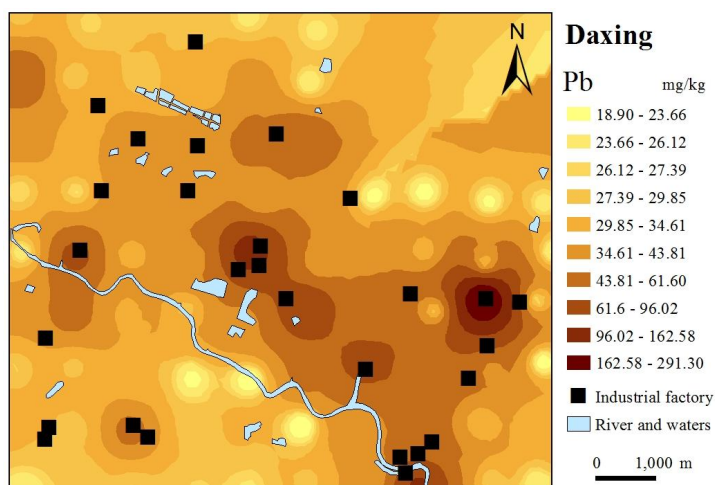
408
 409 **Fig. 2.** Histograms showing the distribution of Cu (a), Pb (b), Zn (c), Cd (d), As (e) and Hg (f)
 410 concentrations within soils from the towns of Daxing and Yicheng.



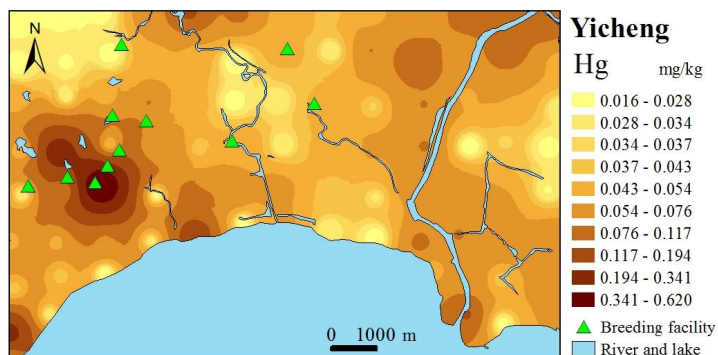
411

412 **Fig. 3.** Multifractal spectra $f(\alpha)$ vs α for soil samples analyzed during this study, showing the
413 multifractal characteristics within all datasets barring the Cu data from the Yichen area, which
414 gives a good indication of the behavior of a metal with typical (i.e. non-anthropogenic)
415 background concentrations.

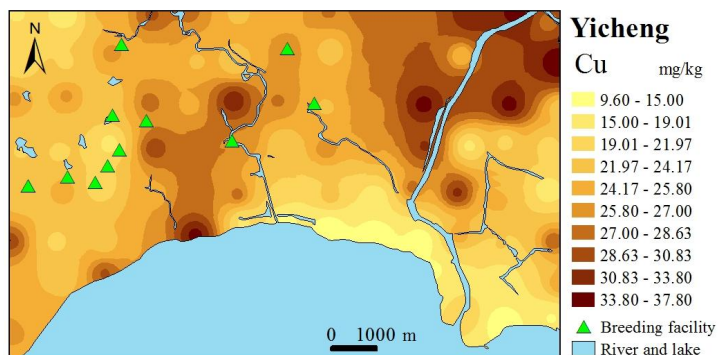
416



417
418 **Fig. 4.** Filled contour maps produced by inverse distance weighted interpolation showing the
419 spatial distribution of Pb in the Daxing area and the clear correlation between Pb contamination
420 and the location of heavy industry.



421
422 **Fig. 5.** Filled contour maps produced by inverse distance weighted interpolation showing the
423 spatial distribution of Hg and the clear spatial relationship with the location of breeding facilities
424 in the Yicheng area.



425
426 **Fig. 6.** Filled contour maps produced by inverse distance weighted interpolation showing the
427 spatial distribution of Cu and the location of breeding facilities in the Yicheng area; this
428 distribution shows that the distribution of Cu in soils in this region is unlike the Hg contamination
429 in this area.